Appendix 1 to Clark SM, Pocivavsek A, Nicholson JD, et al. Reduced kynurenine pathway metabolism and cytokine expression in the prefrontal cortex of depressed individuals. *J Psychiatry Neurosci* 2016.

DOI: 10.1503/jpn.150226

Online appendices are unedited and posted as supplied by the authors.

Reduced Kynurenine Pathway Metabolism and Cytokine Expression in the Prefrontal Cortex of Depressed Individuals

Supplementary Information (Online-Only)

1) **Supplemental Methods:**

RNA extraction, purification and quality control:
Total RNA was isolated from approximately 100 mg of frozen brain tissue by a phenol-chloroform-alcohol method using Trizol (Life Technologies Corp., NY, USA). Quantification of the concentration and quality of the extraction was assessed with a Nanodrop instrument and evaluated by the 260/280 and the 260/230 ratio. The quality of the isolated RNA was further assessed by electrophoresis using a formalin-based agarose gel to confirm integrity of the 18S and 28S ribosomal bands. After these steps, 5 mg of total RNA per case were digested with DNAse I to remove potential genomic contamination. Total RNA was re-analyzed by gel electrophoresis, re-quantified with the Nanodrop instrument, and subsequently analyzed with the Agilent 2100 Bioanalyzer (Agilent Technologies, Santa Clara, CA, USA). All RNA samples showed clearly defined 28S and 18S ribosomal bands after DNAse treatment, and the mean ribosomal RNA ratio (28S/18S) was 1.60.

Real-Time RT-PCR:
Five hundred ng of total RNA per sample were reverse transcribed into cDNA in a 20 µl reaction volume using the iScript cDNA Synthesis Kit (Bio-Rad, Hercules, CA, USA) according to the manufacturer's instructions. The cDNA product was diluted in ultrapure water (1:4) and the real-time PCR reaction was conducted using the iQ SYBR Green Supermix (Bio-Rad) in 25 µl total volume using 2 µl of the cDNA preparation. The real-time PCR reaction was run on a MyiQ instrument (Bio-Rad) with a three step cycling program as follows: an initial hot start for 5 min at 95° C followed by 40 cycles with a denaturation step of 15 sec at 95° C, an annealing step of 30 sec at 55° C, and an extension step of 30 sec at 72 °C with the optics on at this last step. In preparation of a melt curve, the samples were heated for 1 min at 95 °C and then cooled for 1 min at 55°C; the melt curve was executed in 10 sec increments of 0.5 °C with the temperature increasing from 55 °C to 95 °C with the optics on.
At least three primer sets per gene were designed using Accelrys Gene 2.0 (Accelrys, Inc., San Diego, CA, USA). Each primer set was tested, and those determined to have the best efficiency according to the reaction conditions previously described were used for quantification. All the selected primer sets generated a single melting peak and were further analyzed by gel electrophoresis to confirm a single amplification product. A total of 21 genes, including four control genes, were analyzed in duplicate using five independent cDNA preparations, in which all four controls genes were run. The primer sets used are listed in Table S1.

Data generation for real-time RT-PCR:
Relative expression was determined using the 2-ΔΔCt method established by Schmittgen and Livak (39). The geometric mean for normalization consisted of the average of four control genes (ribosomal 18S, GAPDH, actin-beta, and RPS17; Supplemental Table 2). The averaged geometric mean of cycle threshold (ct) was 15.29 ± 0.75 SD for control cases and 15.94 ± 1.20 SD for depressed cases. No statistical differences were observed when comparing the geometric mean values of control and depressed cases, confirming adequacy for further quantification. Each cycle threshold of the target gene was normalized with respect to the corresponding geometric mean, and the relative expression was calculated by comparing normalized cycle threshold values with respect to the mean value of the controls. Each individual sample, including those of the control cases, was analyzed with respect to the mean value of the controls using the 2-ΔΔCt algorithm, generating a representative value of fold increase (>1) or decrease (<1).
Before data generation, all the samples were analyzed on their melting curves and those samples with 2 or more melting peaks were further examined by gel electrophoresis. All those amplification products presenting more than a single amplification product or a non-detectable band (smears) were excluded of the analysis for that particular gene. Not all the samples that presented 2 peaks for one gene did so for another and some genes produced more samples with multiple peaks than other genes. This percentage was comparable in controls and depressed cases.

Chemicals and gases:
KYNA, 3-HK, QUIN, L-tryptophan (TRP), [2H6]-L-kynurenine, pentafluoropropionic anhydride (PFPA) and 2,2,3,3,3-pentafluoro-1-propanol (PFP) were obtained from Sigma-Aldrich (St. Louis, MO, USA). L-Kynurenine sulfate ("kynurenine"; purity: 99.4%) was obtained from Sai Advantium (Hyderabad, India). [2H3]-QUIN was purchased from Synfine Research (Richmond Hill, Ontario, Canada), and [2H5]-TRP was obtained from CDN Isotopes (Pointe-Claire, Quebec, Canada). Other chemicals were obtained from a variety of suppliers and were of the highest commercially available purity. Helium, nitrogen and methane (all 99.999% purity) were obtained from Airgas (Salem, NH, USA).

KYNA and 3-HK determination:
On the day of the assay, tissues were weighed while frozen and then homogenized (1:10, wt/vol) by sonication in ultrapure water. Two hundred µl of the homogenate were then acidified with 50 µl of 6% perchloric acid. After centrifugation (12,000 x g, 10 min), 20 µl of the supernatant were analyzed by HPLC to detect either KYNA or 3-HK.

KYNA was isocratically eluted from a 3 µm C18 reverse-phase column (80 mm x 4.6 mm; ESA, Chelmsford, MA, USA), using a mobile phase containing 250 mM zinc acetate, 50 mM sodium acetate, and 3% acetonitrile (pH adjusted to 6.2 with glacial acetic acid), at a flow rate of 1.0 ml/min. KYNA was detected fluorimetrically in the eluate (excitation: 344 nm, emission: 398 nm; Perkin Elmer Series 200 fluorescence detector, Waltham, MA, USA) at a retention time of approximately 7 min.
3-HK was eluted from a 3 µm HPLC column (HR-80; 80 mm x 4.6 mm; ESA), using a mobile phase consisting of 1.5 % acetonitrile, 0.9 % triethylamine, 0.59 % phosphoric acid, 0.27 mM EDTA, and 8.9 mM sodium heptane sulfonic acid, at a flow rate of 0.5 ml/min. 3-HK was detected electrochemically in the eluate using a HTEC 500 detector (Eicom Corp., San Diego, CA, USA; oxidation potential: + 0.5 V). The retention time of 3-HK was approximately 11 min.

TRP, kynurenine and QUIN measurement:
TRP, kynurenine and QUIN levels in the brain were quantified by GC/MS. Tissue was homogenized (1:20, wt/vol) in an aqueous solution containing 0.1% ascorbic acid. Fifty µl of a solution containing internal standards (500 nM [2H5]-TRP, 10 µM [2H6]-L-kynurenine and 50 nM [2H3]-QUIN) were added to 50 µl of the tissue preparation, and proteins were precipitated with 50 µl of acetone. After centrifugation (13,700 x g, 5 min), 50 µl of a methanol:chloroform mixture (20:50, vol/vol) were added to the supernatant, and the samples were centrifuged (13,700 x g, 10 min). The upper layer was added to a glass tube and allowed to evaporate to dryness (90 min). The samples were then incubated with 120 µl of PFP and 130 µl of PFPA at 75° C for 30 min, dried down again, and taken up in 50 µl of ethyl acetate. One µl was then injected into the GC. GC/MS analysis was carried out with a 7890A GC coupled to a 7000 MS/MS (Agilent Technologies, Wilmington, DE, USA), using electron capture negative chemical ionization.

Histology and immunohistochemistry:
Serial consecutive sections were processed for microscopic histological analyses as follows: 1) Nissl staining to delineate gray and white matter integrity; 2) Hematoxylin and Eosin staining for the assessment of vascular integrity and verification of the absence of peripheral cell infiltration; 3) Acidic Toluidine blue staining to detect mast cells and corpora amylacea indicative of dead astrocytes and normal aging processes; 4) Iba1 immunohistochemistry to assess microglia activation by morphological analysis. In all cases, sections were brought to room temperature under vacuum and fixed for 20-30 min in a 4% solution of paraformaldehyde in phosphate buffered saline (PBS). The sections were then washed with PBS or

Tris-buffered saline (TBS) and processed for histology or immunohistochemistry.
Immunohistochemistry was carried out using the nickel-DAB method for enhanced detection of signal and higher contrast. After fixation, the slide-mounted sections were washed twice in PBS followed by 15 min incubation with 1% H2O2 in PBS to inactivate endogenous peroxidase. The sections were incubated in a humidification chamber with 1:100 dilution of anti-Iba1 IgG (Cat #019-19741, Wako Chemicals, Richmond, VA) in 0.2% Triton X 100 (Sigma-Aldrich) in PBS (PBST) buffer for 1 hour at room temperature followed by overnight incubation at 4 °C under gentle agitation. The slides were then washed 3 times in PBST for 1 hour followed by one hour incubation with HRP conjugated goat anti-rabbit IgG (Cat #: 554021, BD Biosciences, San Jose, CA) in PBST at room temperature. The sections were washed 3 times in PBS for 1 hour followed by a 5 min incubation in 0.175 M sodium acetate solution (pH 7.4) and further incubated in 3,3'-diaminobenzidine (DAB) (Sigma-Aldrich) and nickel sulfate heptahydrate (Sigma-Aldrich) in 0.175 M sodium acetate solution. The nickel sulfate and the DAB co-precipitate result in a dark gray signal that is readily detectable over background.

Semiquantitative analysis of microglia using Iba1 staining: Preliminary analyses indicated that Iba1 staining produced positive signals in both microglia within the parenchyma of the brain and in macrophages within vascular and meningeal spaces. The Iba1 signal in the parenchyma was sufficient to allow for the identification of microglia according to their morphology. Semi-quantification of these cells was performed manually by two blinded observers and expressed as number of cells per cm2. In brief, digital images were taken at 100X magnification, and cell counting was carried out by classifying microglia as shown in Figure S1 as ramified with long thin processes (S1A), intermediate with shorter and thickened basal processes (S1B), and amoeboid with very short thick processes with round soma (S1C). The total number of microglia as well as the number of amoeboid cells were calculated and used for comparisons. Hypertrophic microglial cells as shown in figure S1D were also identified. Due to the difficulty to delineate their cellular boundaries and associations with other Iba1 positive cells, they were excluded from analysis. Nevertheless, the frequency of cases presenting these structures was compared between control and depressed cases.

2) Table S1:

Gene	Accession	Forward	Reverse	Amplicon (bp)	Position	Region	Ave (ct)
IDO1	NM_002164	TGCCCCTGTGATAAACTGTGGTC	CCATAGCGTGTGCCATTCTTGTAG	120	11-130	Exon 1	26.3
IDO2	NM_194294	TGGATGGAAAGACAACCCAG	TTGCTATGACGAATGCCTAAG	144	998-1141	Exons 9-10	28.4
TDO2	NM_005651	AACCTCCGTGCTTCTCAGAC	CCTCCTTTGCTGGCTCTATTC	150	33-182	Exons 1-2	25.5
KMO	NM_003679	TTTCTTCCTGTTGCCTGCCC	CCAAGCAGTCTTCAAAGCCC	149	1139-1287	Exons 10-11	21.2
KAT II	NM_016228	CCAGCACTTTTAACCAGCTC	CCAAACCAGTTAACCACTTGTC	150	1226-1375	Exons 9-11	24.1
IL1-β	NM_00576	GCACCTTCTTTCCCTTCATCTTTG	GCTTTTTTGCTGTGAGTCCCG	128	359-486	Exons 4-5	29.7
IL2	NM_000586	TCACAGTAACCTCAACTCCTGC	GTGCAAGACTTAGTGCAATGC	72	30-101	Exon 1	34.8
IL4	NM_000589	AAGCAAAAAGCCAGCAGCAGCC	ACAAAGTTTCAGCATAGGAAATTAC	85	10-94	Exon 1	24.6
IL5	NM_000879	GCACTGCTTTCTACTCATCG	CCTTGCACAGTTTGACTCTC	140	147-286	Exons 1-3	33.5
IL6	NM_000600	GAGAAGATTCCAAAGATGTAGCCG	AGATGCCGTCGAGGATGTACC	96	214-309	Exon 2	30.2
IL13	NM_002188	ACCCACTTCACACACAGGCAAC	ACAGTCTTCCCCAATCCCCAAC	125	794-918	Exon 4	26.6
IL33	NM_033439	TGAAAAACCACTGCCAGAC	ACTCAACCCAAGACTCACAG	221	702-922	Exon 8	25.6
IFN-γ	NM_000619	CAGTTAAGTCCTTTGGACCTG	CAGCCAAGAGAACCCAAAAC	142	47-188	Exon 1	29.2
TNF-α	NM_000594	AAGCAACAAGACCACCACTTCG	TCTCCAGATTCCAGATGTCAGGG	148	1016-1163	Exon 4	31.1
CCL2	NM_002982	CATAGCAGCCACCTTCATTC	CAGCTTCTTTGGGACACTTG	155	109-263	Exons 1-2	25.8
COX2	NM_000963	GCTGGGAAGCCTTCTCTAAC	GCTGGGCAAAGAATGCAAAC	198	508-705	Exons 4-5	26.4
18S	K03432	CCGATAACGAACGAGACTCTGG	TGAACGCCACTTGTCCCTCTAAG	93	1374-1466	rRNA	11.5
ACTB	NM_001101	CCACGAAACTACCTTCAACTC	AGTGATCTCCTTCTGCATCC	133	906-1038	Exon 5	18.5
GAPDH	NM_002046	TTCGTCATGGGTGTGAACC	TGGTCATGAGTCCTTCCAC	139	493-631	Exons 5-6	17.4
RPS17	NM_001021	CCTGACACTAAGGAAATGCTGAAG	AAAATTCAAACAGGTCCCCGAG	116	327-442	Exons 4-5	22.4

Table legend:
Primer set used in RT-PCR determinations. The primer sets listed were selected based on optimal reaction efficiency using the same amplification conditions for all primers. IDO1, IDO2: indoleamine-2,3-dioxygenase genes 1 and 2; TDO2: tryptophan-2,3-dioxygenase; KMO: kynurenine 3-monooxygenase (kynurenine 3-hydroxylase); KAT II: α-aminoadipate aminotransferase (AADAT) transcript variant 1; IL: interleukins; IFN-γ: interferon gamma; TNF-α: tumor necrosis factor alpha; CCL2: chemokine (C-C motif) ligand 2; COX2: prostaglandin-endoperoxide synthase 2; GAPDH: glyceraldehyde-3-phosphate dehydrogenase transcript variant 1; ACTB: actin beta; RPS17: ribosomal protein S17; 18S: ribosomal 18s gene; Ave (ct): Average threshold cycle for all the cases studied indicating relative abundance of the difference mRNA species.

3) Table S2:

Pearson correlations coefficients (r) between KP metabolites and gene expression of KP enzymes in a pooled sample of N = 32 Control and N = 43 Depressed individuals

		IDO1	IDO2	TDO2	KATII	KMO	KYNA	3-HK	QUIN
Kynurenine	r	0.126	0.160	0.114	-0.214	-0.166	0.480	0.508	0.580
	p-value	*0.281*	*0.198*	*0.332*	*0.067*	*0.153*	***<0.0001***	***<0.0001***	***<0.0001***
Kynurenine/TRP	r	0.245	0.327	0.279	0.061	0.024	0.435	0.415	0.249
	p-value	***0.034***	***0.008***	***0.015***	*0.604*	*0.841*	***<0.0001***	***<0.0001***	***0.025***
KYNA	r	0.051	0.060	0.021	-0.030	-0.127		*0.769*	0.634
	p-value	*0.665*	*0.630*	*0.858*	*0.797*	*0.279*		***<0.0001***	***<0.0001***
3-HK	r	0.046	0.059	0.054	-0.041	-0.209	0.769		0.628
	p-value	*0.693*	*0.638*	*0.647*	*0.731*	*0.072*	***<0.0001***		***<0.0001***
QUIN	r	0.239	0.174	0.166	-0.061	-0.027	0.634	0.628	
	p-value	*0.039*	*0.163*	*0.156*	*0.606*	*0.820*	***<0.0001***	***<0.0001***	

4) Table S3:

Evaluation of the effect of antidepressant treatment on KP metabolites

	Control	Fluoxetine	
	Mean ± SEM		*P-value*
TRP pmoles/mg tissue	38.1 ± 1.4	41.0 ± 1.1	0.137
Kynurenine pmoles/mg tissue	2.2 ± 0.2	2.2 ± 0.1	0.836
KYNA fmoles/mg tissue	20.7 ± 3.4	20.3 ± 2.5	0.922
3-HK fmoles/mg tissue	9.2 ± 1.2	8.4 ± 1.7	0.689
QUIN fmoles/mg tissue	119.7 ± 3.6	118.5 ± 2.9	0.799

Table legend:

Sixteen male Sprague-Dawley rats (200-250 grams; Charles River Laboratories) were kept in a temperature-regulated room (22 ± 1°C), on a 12 h light/12 h dark cycle, two per cage, with food and water *ad libitum.* Fluoxetine (fluoxetine HCl; Silarx Pharmaceuticals, Inc.; Spring Valley, NY) was administered via drinking water so that animals received ~10 mg/kg/day for 21 consecutive days. At the completion of treatment, animals were euthanized via CO_2 inhalation and the brain was collected for biochemical analysis of KP metabolites. Briefly, on the day of the assay, the cortex was thawed and sonicated in ultrapure water (1:5 w/v for 3-HK analysis, 1:10 w/v for KYNA analysis, 1:20 w/v for TRP, kynurenine and QUIN). Metabolites were determined by HPLC or GC/MS as described in Materials and Methods. These experiments were approved by the Institutional Animal Care

and Use Committee (IACUC) of the University of Maryland School of Medicine.

5) Figure S1

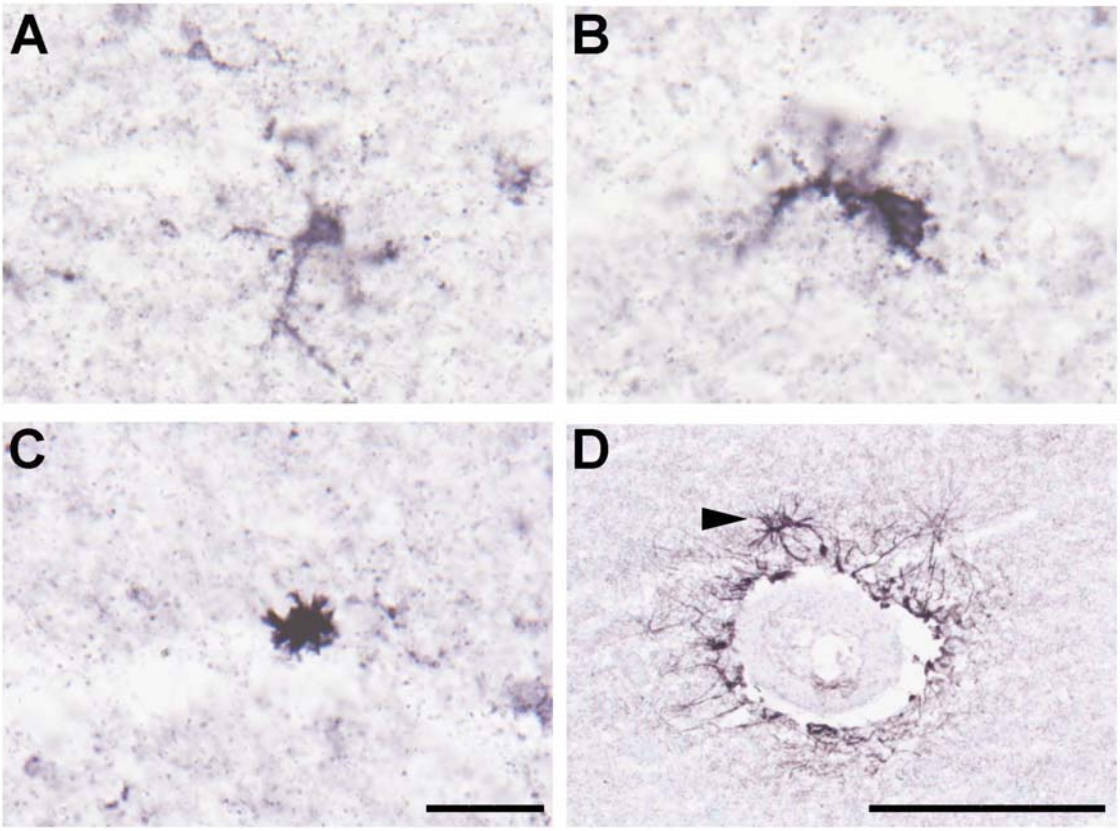

Figure legend:

Representative digital microphotographs of Iba1-stained microglial cells in the VLPFC showing different morphologies A: Ramified microglia with thin processes, B: Intermediate microglia with enlarged basal processes and shorter ramifications, C: Amoeboid microglia with a rounded soma and retracted processes. D: Hypertrophic microglia (arrowhead) surrounding a possible protein aggregate in the parenchyma of the gray matter. Scale bars: A to C = 20 µm; D = 100 µm.

6) Figure S2

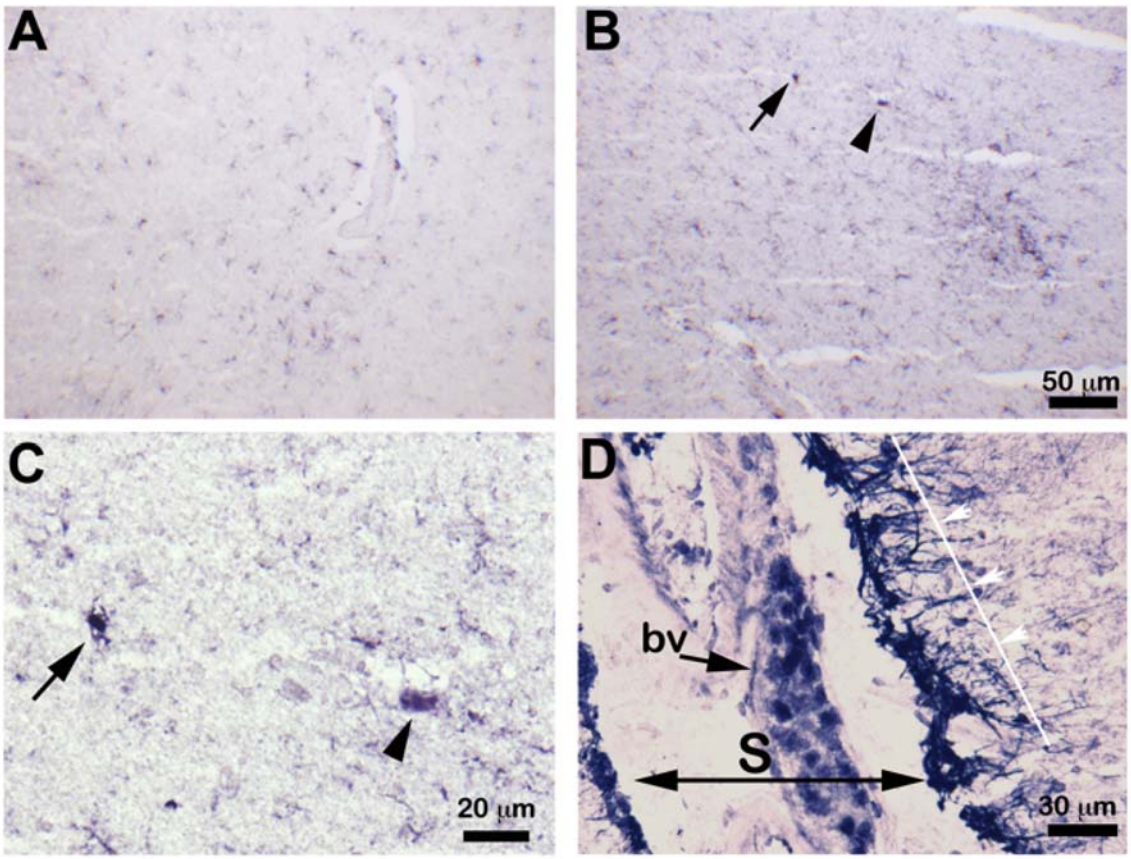

Figure legend:

Representative digital microphotograph of IBA1-stained microglial cells at 100X magnification used for semi-quantification of microglia in control (A) and depressed (B) cases. The arrow in panel B indicates the only identified amoeboid microglia in these fields that at higher magnification (panel C; 200X) presented a clear round shape with short ramified processes. The arrowhead shows a lightly stained IBA1-positive cell without clear processes and which was therefore excluded from microglial quantification. The white line with white arrows in panel D shows hypertrophic microglia lining the borders of a sulcus (S). Note the presence of IBA1-positive macrophages inside a blood vessel (bv) of the sulcus.

7) Figure S3

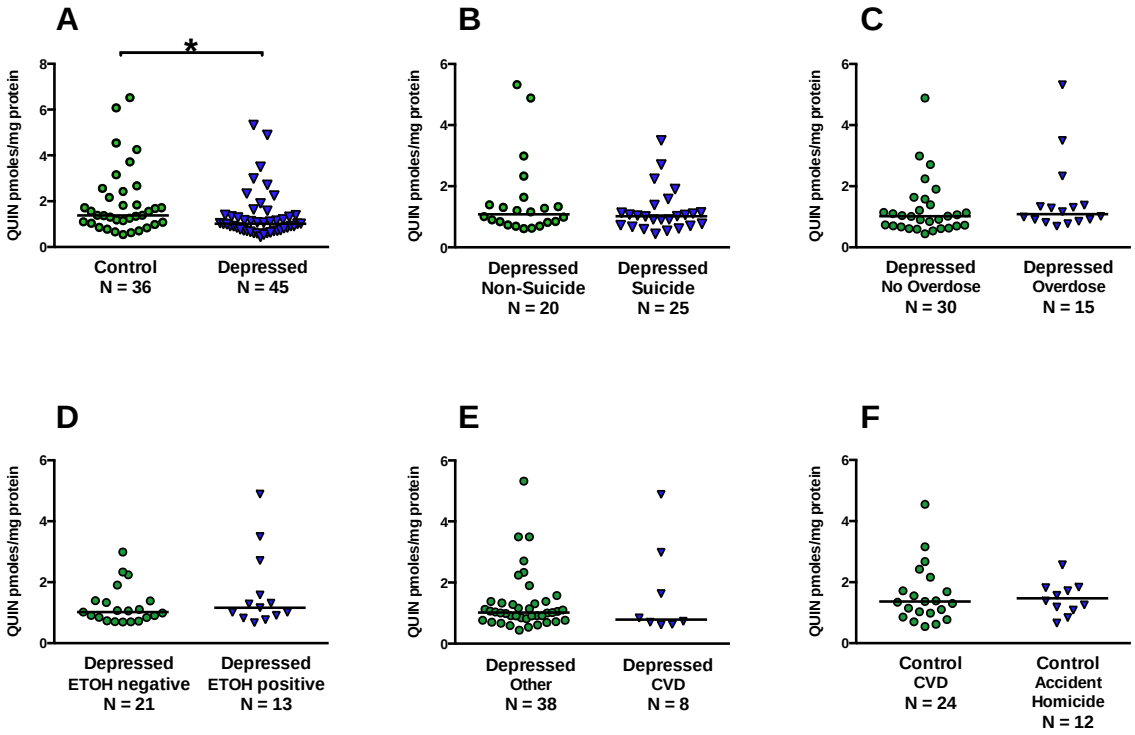

Figure legend:

Subgroup comparisons of non-transformed values for QUIN levels in the VLPFC. Shown are scatter plots with median of control and depressed cases (A); depressed individuals that died by suicide *vs.* non-suicide (B); depressed individuals that died by overdose *vs.* no overdose (C) depressed individuals positive for alcohol *vs.* negative for alcohol at the time of death (D); depressed individuals that died by cardiovascular related events *vs.* other (E); and control non-psychiatric cases that died by cardiovascular related events *vs.* accident and homicide (F). * Wilcoxon test, z = 2.57, df = 1, p = 0.01

8) Additional Subgroup analyses

Exploratory subgroup analysis for the kynurenine/TRP ratio indicated no significant difference between groups for: depressed suicide (n = 25) *vs.* non-suicide (n = 20); adjusted geometric mean, suicide = 0.0361 *vs.* non-suicide = 0.0374; t = 1.09, df = 39, p = 0.625), depressed overdose (n = 15) *vs.* depressed non-overdose (n = 30); adjusted geometric mean overdose = 0.0382 *vs.* non-overdose = 0.0389; t = 0.46, df = 39, p = 0.645). Two-way analysis of covariance ANCOVA was used to examine the relationship of cardiovascular (CVD) versus non-CVD deaths on differences between depressed and control cases. There was no statistically significant interaction between depression status and CVD versus non-CVD cause of death in their effects on the kynurenine/TRP ratio (F = 1.05, df = 1,72, 0.31). When adjusting for CVD versus non-CVD death, age, PMI and gender, the geometric means for the kynurenine/TRP ratio were 0.045 in controls and 0.039 in depressed, F = 2.59, df = 1,72, p = 0.11). Adjusted subgroup geometric means were control non-CVD = 0.046, control CVD = 0.044, depressed non-CVD = 0.037, depressed CVD = 0.042.
Furthermore, no subgroup differences were observed for TRP or kynurenine levels. Similarly, no subgroup differences were found for QUIN and the enzymes IDO1, IDO2 and TDO. Additional subgroups comparisons for cytokines showed no significant differences.